Impacts of Soil and Antenna Characteristics on LoRa in Internet of Underground Things

Baofeng Zhou, Venkat Sai Suman Lamba Karanam, Mehmet C. Vuran
Cyber-Physical Networking Laboratory
Department of Computer Science & Engineering
University of Nebraska-Lincoln, Lincoln, NE 68588
Email: {bzhou, saisuman}@huskers.unl.edu, mcv@unl.edu

GLOBECOM 2021 - 2021 IEEE Global Communications Conference | 978-1-7281-8104-2/21/$31.00 ©2021 IEEE | DOI: 10.1109/GLOBECOM46510.2021.9685610

***Abstract*—Long-range (LoRa) is a suitable candidate for underground wireless communications due to its capability of communicating over a long range. However, due to the uniqueness of soil properties at a given geographical location, and the varying nature of soil moisture, it is challenging to apply a universal approach to characterize LoRa in wireless underground channels. In this paper, the performance of LoRa in underground channels is studied both theoretically and empirically. The range and bit error rate (BER) formulation of LoRa is derived as a function of soil parameters based on statistical underground channel models. To validate the model, path loss measurements are conducted under different moisture levels in two soil types (sandy and silty clay loam soil). In addition, as underground communication is also dependent on the return loss of buried antennas, the path loss measurements are performed using two different types of underground antennas. Results show that the underground channel models agree well with empirical LoRa measurements, resulting in R-squared values of 0.87-0.89. The results suggest that the performance of LoRa in underground channels can be predicted using the models developed in this paper.**

I. Introduction

The Internet of Underground Things (IoUT) [1], [2] is an emerging technology for connecting underground sensors, enabling applications such as smart irrigation, precision agriculture, smart city infrastructure, tunnel, flood monitoring systems, and surveillance systems. Soil is a dielectric medium with several properties affecting its permittivity, including soil texture, soil bulk density, and soil water content. The combined effects of these diverse factors introduce a unique interaction between UG communication systems and the soil medium. Therefore, the communication range and quality through underground (UG) channels need to be characterized as a function of these factors.

Recently, research communities have shown a growing interest in using Low Power Wide Area Networks (LPWAN) technique, i.e., LoRa, in underground sensor networks due to its low-power, low-cost, and long-range communication capabilities. Most related recent efforts have focused on the experimental characterization of LoRa in underground sensor networks. Results have shown that LoRa is suitable for forming underground sensor networks, and the transmission distance can reach up to 200m [3]–[6]. In [3], the performance of LoRa in the underground to underground (UG2UG) and underground to aboveground (UG2AG) channels is observed at the 433MHz frequency band through measurements in multiple types of soil. The correlation between received signal strength indicator (RSSI) and signal-to-noise ratio (SNR) and buried antenna depth and transmission power, and soil properties such as particle distribution, bulk density, or Volumetric Water Content (VWC), are evaluated through extensive measurement at various soil sites. In [4]–[6], similar results are reported to characterize the RSSI, SNR, and Packet Delivery Ratio (PDR) in UG2AG and aboveground to underground (AG2UG) links under varying buried depths. However, in these studies, the impact of soil moisture variation is challenging to capture because the soil moisture is uncontrollable in natural environments. Moreover, the effects of soil on buried antennas are not considered in existing analyses.

In this paper, we aim to facilitate a universal approach that models the impact of soil characteristics on LoRa and complement existing investigations by incorporating the effects of the underground antenna performance on LoRa transmissions. This is important to further accurately describe the applicability of LoRa in underground communications, especially under varying soil conditions. Therefore, we utilize established underground channel and antenna models to analyze the performance of LoRa. Subsequently, we validate the derived models through empirical measurements in several soil conditions and settings. The contributions of this paper are as follows: (1) The theoretical range, data rate, and bit error rate (BER) of LoRa are captured based on statistical underground channels. We focus on analyzing the range and BER performance of LoRa under varying soil conditions. (2) Experiments are conducted to validate the channel and performance models. The path loss and antenna return loss are measured in two different soil types in indoor and outdoor environments. We also measure LoRa performance under controlled soil moisture at dry and wet conditions using dipole and wideband micropatch antennas.

The rest of the paper is organized as follows: The background of soil-dependent wireless underground channel models are discussed in Section II. LoRa and its performance in underground channels are analyzed in Section III. Empirical evaluations are described in Section IV. The paper is concluded Section V.

II. Background

In this section, we summarize the UG channel characteristics and associated models, upon which the rest of the paper

978-1-7281-8104-2/21/$31.00 ©2021 IEEE

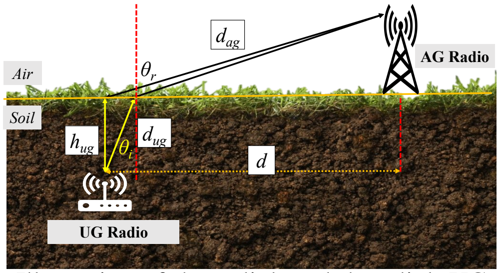

Fig. 1: Illustration of the uplink and downlink UG channels.

builds.

A. Underground Link Budget

The uplink (UG2AG) and downlink (AG2UG) communication channels are depicted in Fig. 1, the models of which were developed in [7], [8]. Both links are composed of two path components: the UG component in soil and the AG component in air. Based on the path loss characterization of the UG channel, the link budget of the channel is modeled as follows [9], [10]:

$$P_{rx} = P_{tx} + G_A + 10\log_{10}\left(1 - 10^{-\frac{RL_{ug}}{10}}\right) - PL, \quad (1)$$

where P_{rx} is the received signal power, P_{tx} is the transmit signal power, G_A is the sum of gains of the transmit and receive antennas, RL_{ug} is the power loss caused by underground antenna return loss, and PL is the path loss of the underground channel.

B. UG Channel Path Loss Model

Based on the channel model depicted in Fig. 1, the path loss of UG channels includes three loss components, (1) the path loss in the soil medium (PL_{UG}), (2) the refraction loss due to the soil-air interface ($L_{R,\rightarrow}$) based on the link direction (uplink or downlink), and (3) the path loss in the air (PL_{OTA}) [7]:

$$PL_{\rightarrow}[dB] = PL_{UG}(d_{ug}) + PL_{OTA}(d_{ag}) + L_{R,\rightarrow}, \quad (2)$$

where the subscript $\rightarrow$ refers to the communication direction (downlink [DL] or uplink [UL]), d_{ug} and d_{ag} are the lengths of the underground and OTA portions of the wireless signal path, respectively, and each component is given as follows [7], [11], [12]:

$$PL_{UG}(d_{ug}) \simeq 6.4 + 20log(d_{ug}) + 20log(\beta) + 8.69\alpha d_{ug},$$

$$PL_{OTA}(d_{ag}) \simeq -147.6 + 10\eta\log(d_{ag}) + 20\log(f),$$

$$L_{R,DL} \simeq 10log\frac{\left(cos\theta_I + \sqrt{\epsilon'_s - sin^2\theta_I}\right)^2}{4cos\theta_I\sqrt{\epsilon'_s - \sin^2\theta_I}},$$

$$L_{R,UL} \simeq 10log(\sqrt{\epsilon'_s} + 1)^2/(4\sqrt{\epsilon'_s}),$$

where α and β determine the attenuation and phase shift of the wave in soil, respectively, η is the OTA attenuation coefficient that has been empirically characterized to be around 2.8 to 3.3 due to reflections and attenuation [8], d_{ag} is the distance between the refraction point and the AG node, f is the carrier frequency of the signal, ϵ'_s is the real part of the relative dielectric constant of the soil-water mixture and θ_I is the incident angle based on Snell's law. Refraction constitutes the main difference between uplink and downlink channels. It can be observed that uplink refraction loss does not depend on the incident angle, θ_I.

The propagation of the signal in the soil is affected by the soil medium and determined by the soil dielectric properties, i.e., soil permittivity. Due to the higher relative permittivity of soil than that of air and the varying nature of soil properties (e.g., *soil moisture, soil bulk density, and soil textural composition*) that determines the permittivity, it is crucial to characterize the impact of soil permittivity in the channels as we discuss next.

C. Soil Dielectric Properties

The complex-valued soil permittivity can be considered as $\epsilon_s = \epsilon'_s - i\epsilon''_s$, where ϵ'_s and ϵ''_s are the real and imaginary parts of the relative soil permittivity and are both empirically characterized in the frequency range of 0.3–1.3GHz as [13]:

$$\epsilon'_s = 1.15\left[1 + \frac{\rho_b}{\rho_s}\left(\epsilon_s^{\delta} - 1\right) + (m_v)^{v'}\left(\epsilon'_{fw}\right)^{\delta} - m_v\right]^{\frac{1}{\delta}} - 0.68, \quad (3)$$

$$\epsilon''_s = \left[(m_v)^{v''}(\epsilon''_{fw})^{\delta}\right]^{\frac{1}{\delta}}, \quad (4)$$

where ρ_b and ρ_s are the bulk density and particle density of the soil, respectively, $\epsilon_s = (1.01 + 0.44\rho_s)^2 - 0.062$ is the dielectric constant of the soil solids, m_v is the volumetric water content, δ, v', and v'' are empirically determined soil-type dependent constants given by:

$$\delta = 0.65, \quad v' = 1.2748 - 0.519S - 0.152C,$$

$$v'' = 1.33797 - 0.603S - 0.166C,$$

where S and C are the fractions of sand and clay composing the soil mixture, respectively; ϵ'_{fw} and ϵ''_{fw} are the real and imaginary parts of the relative dielectric constant of water that can be found in [1], [13]. Based on soil permittivity, ϵ_s, the propagation wave number of EM waves in the soil can be considered as $k_s = \beta + i\alpha = \omega\sqrt{\mu\epsilon_s}$, where α and β are determined by [14]:

$$\alpha = \omega\sqrt{\frac{\mu\epsilon'_s}{2}\left[\sqrt{1 + \left(\frac{\epsilon''_s}{\epsilon'_s}\right)^2} - 1\right]}, \quad (5)$$

$$\beta = \omega\sqrt{\frac{\mu\epsilon'_s}{2}\left[\sqrt{1 + \left(\frac{\epsilon''_s}{\epsilon'_s}\right)^2} + 1\right]}, \quad (6)$$

where ω is the angular frequency and μ is the magnetic permeability of soil.

D. Antenna Return Loss Variation

Also affecting the link budget of the channel in (1) is the variations of return loss, RL_{ug}, in buried dipole antennas, which has been modeled and validated in [9], [15]. The effect is caused by the impedance mismatch of the antenna jointly determined by soil permittivity changes and reflection from the soil-air interface at a given depth. According to the

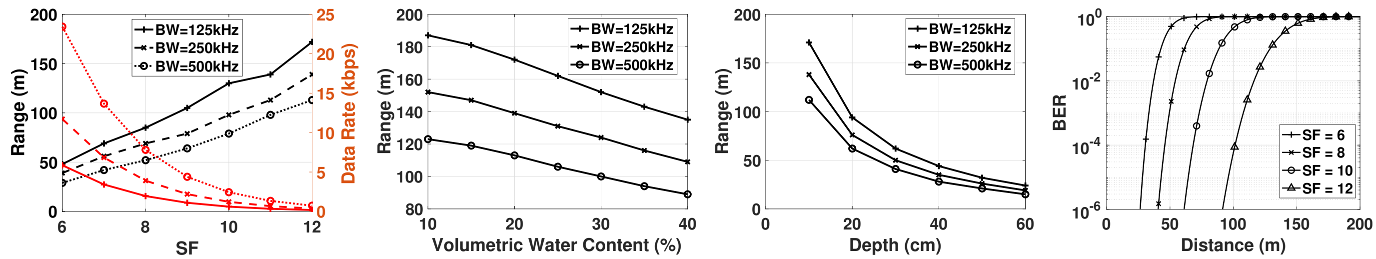

(a) (b) (c) (d)

Fig. 2: (a) The theoretically achievable range and data rate of LoRa in UG2AG channel. (b) The impact of soil moisture on the maximum range. (c) The impact of buried depth on the the maximum range. (d) The BER of UG2AG channel versus distance.

dipole antenna return loss model developed in [9], the resonant frequency, f_r, can be found by [15]:

$$f_r = \max_f \left(RL_{ug}(f) \right), \tag{7}$$

where $RL_{ug}(f)$ is the return loss of the underground antenna in dB as a function of frequency, f, which is generally empirically characterized and theoretical models exist [15]. An antenna matched in the air to operate at a designated frequency f_{OTA} will have a different resonant frequency $f_r < f_{OTA}$ when deployed in soil. This shift introduces additional signal loss at the carrier frequency of f_{OTA} due to the higher antenna return loss.

Combining (2)-(7) within (1), the key observations are that the signal experiences higher attenuation at high soil moisture levels, large deployment depth, and the high percentage of sand. It is also favorable to utilize lower frequency bands to extend the communication range in UG channels.

III. Analysis of the Impact of Soil Medium on LoRa Transmissions

LoRa is a proprietary physical layer technology for LoRaWAN and is based on the chirp spread spectrum (CSS) [10]. LoRa has several key parameters: (1) *Spreading Factor (SF)*: LoRa spreads the information bits into longer bit sequences based on the chosen SF ranging from 7 to 12. Each information bit is spread into 2^{SF} bits. A larger spreading factor offers lower SNR required for the receiver to demodulate the signal. (2) *Bandwidth (BW)*: The bandwidth is the width of the transmitted signal in frequency. The symbol rate can be expressed as $C_S = BW/2^{SF}$. (3) *Coding Rate (CR)*: LoRa utilizes forward error correction based on Hamming code [16]. The coding rate determines the number of redundant bits for error correction.

The underlying challenge in studying the LoRa performance in the underground channel is the lack of comprehensive models that capture the diverse and time-varying nature of soil properties. This impedes applying experimental findings from one location to another due to the deviations in soil composition, soil moisture, and other properties. Therefore, we take a top-down approach to study the performance of LoRa leveraging the modeling of underground channels. Based on the models presented in Section II, we aim to identify and quantify the performance of LoRa in underground communication channels. We derive the performance of LoRa in terms of maximum communication range and BER under varying conditions, including soil moisture, soil composition, and buried depth, facilitating pre-deployment planning and enabling online prediction of LoRa performance in the field.

1) Range and Data Rate of Uplink Transmission: In this section, we focus on the uplink communication due to the constraints in size, power, and antenna options for UG nodes compared to the AG gateway nodes. LoRa promises an extended communication range compared to existing FSK-based modulation schemes. This is enabled by the low sensitivity provided by CSS. As mentioned above, the higher-order spreading factor gives a longer range and results in a lower data rate. The data rate of LoRa is given by [10]:

$$C_b = SF * \frac{4BW}{(4 + CR)2^{SF}}, \tag{8}$$

where SF, CR, and BW are the spreading factor, coding rate, and bandwidth, respectively. Therefore, there is a trade-off between communication range, throughput, and energy consumption when selecting the spreading factor used for transmission. The spreading factor and bandwidth jointly determine the data rate.

We determine the maximum achievable range, R, of the uplink transmission as follows :

$$R(SF, BW) \simeq \max \left\{ d : P_{rx} > P_{sens}(SF, BW) \right\}, \tag{9}$$

where P_{rx} is the received power in (1), $P_{sens}(SF, BW)$ is the receiver sensitivity for a given SF and bandwidth combination.

Plugging in (1) in (9), we characterize the trade-off between range and data rate in the uplink channel. Unless otherwise noted, the default values used in the model are considered as follows: the transmit power is 0 dBm, the UG node burial depth is 40 cm, and the AG node height is 4 m. The soil volumetric water content is 20%, the percentage of sand and clay in the composition are 31% and 29%, respectively. The bulk density and particle density of soil are 1.85 g/cm^3 and 2.66 g/cm^3. We consider a typical 6 dB fading margin, 3 dB cable and connection losses, and 4 dB in noise figure introduced by the electronic components in both transmitter and receiver to approximate a practical setting. The trade-off between range and data rate based on the SF and BW selection are shown in Fig. 2a. For example, when the UG node is configured with SF=11 and BW=250kHz, switching to SF=12

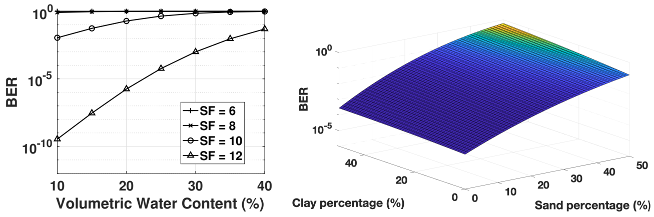

(a) (b)

Fig. 3: The BER model of UG2AG channel versus: (a) volumetric water content ($d = 100$m), and (b) soil textual composition.

can improve the range by 23%. Consequently, the data rate decreases because of the change in modulation order.

The impacts of soil moisture and buried depth on the communication range of LoRa are shown in Fig. 2b and 2c, respectively . As shown in Fig. 2b, a 10% increase in VWC, reduces the range by at least 6%. Therefore, deployment planning should consider the temporal soil moisture variations to determine a worst-case distance to the gateway to avoid loss of connectivity. Similarly, it is shown in Fig. 2c that the range decreases monotonically with the burial depth. When the underground deployment is below 40 cm, it is very challenging for LoRa to achieve ranges over 100 m, even when the SF is configured to 12.

2) Bit Error Rate of LoRa: The BER of LoRa has been modeled as [4], [17], [18]:

$$BER = Q\left(\frac{log_{12}(SF)}{\sqrt{2}}\frac{E_b}{N_0}\right), \tag{10}$$

where E_b/N_0 is the energy per bit to noise power spectral density ratio. Due to the spreading of LoRa modulation, E_b/N_0 of LoRa can be expressed as [4]:

$$\frac{E_b}{N_0} = SNR - 10\log\left(\frac{SF \cdot CR}{2^{SF}}\right), \tag{11}$$

In underground channels, the noise floor has been characterized empirically in [19] to be around -110 dBm/Hz, which is higher than thermal noise in the air. As a result, the SNR can be estimated by $SNR = P_t - PL_{UL} - P_n$, where P_t is the transmit power and P_n is the underground noise power.

The theoretical BER of LoRa in the UG2AG channel is derived based on the channel model. In Fig. 2d, the BER of LoRa is shown as a function of the communication distance. It can be observed that when the link reaches the maximum range , BER increases due to the reduction in SNR. In Fig. 3a, the impact of VWC on BER is illustrated for $d_{ag} = 100m$. Similar to the change in the communication range with respect to soil moisture level, the BER performance of LoRa also degrades with the increase in soil moisture level. Moreover, a high SF value preserves better BER performance. In Fig. 3b, the relationship between BER and soil textual composition is shown for $d_{ag} = 100m$ and $SF = 6$. The main cause for BER to be varying with sand and clay percentage is the change in signal attenuation. Different compositions of soil have distinct permittivity . Therefore, the path loss and SNR are affected .

TABLE I: Soil Parameters

Parameter	Value	Parameter	Value
ρ_s	$2.65gr/cm^3$ [21]	ρ_b	$1.42gr/cm^3$ (sandy) $1.30gr/cm^3$ (silty clay loam) [21]
S	0.86 (sandy) 0.13 (silty clay loam) [14]	C	0.03 (sandy soil) 0.32 (silty clay loam) [14]
m_v	variable	δ	0.65 [14]
v	1.1587	v"	1.2065
ϵ'_{fw}	80.0992	ϵ''_{fw}	$7.4851 * 10^{-6}$
ϵ_{w0}	80.1000	$\epsilon_{w\inf}$	4.9 [14]
ϵ_0	55.263	τ_w	$1.20003 * 10^{-12}$
δ_{eff}	0.4914 [13]	μ	1.0006 [22]
ϵ'_s	12.0102	ϵ''_s	$3.4128e - 07$
λ_s	11.57 cm (sandy), 13.09cm (silty clay loam)		

IV. Empirical Evaluation of LoRa in UG Channels

In this section, the evaluations of the performance of COTS LoRa devices are presented, which were conducted in a controlled indoor testbed and an outdoor testbed [20]. We first describe the experimental setup and methodology, followed by the discussion of results.

A. Experiment Setup and Methodology

1) Indoor Testbed: An indoor testbed that facilitates experiments with controlled soil moisture levels, in the form of a $100"(L) \times 36"(W) \times 48"(D)$ sandbox holding about 90 ft^3 of sandy soil located inside a greenhouse, has been used for conducting experiments. At each depth of 10cm, 20cm, 30cm, and 40cm, a quadband half-wavelength dipole antenna with an over-the-air resonant frequency of 433 MHz and a wideband micropatch planar antenna are deployed with a horizontal separation of 50 cm. The antennas are connected to COTS LoRa devices [23] using ufl to SMA adapters. The height of the aboveground node is 1.66 m. To accurately measure the soil moisture level, two sets of Watermark soil moisture sensors [24] are deployed at these depths at each side of the sandbox. These sensors are connected to a data logger for soil moisture measurements.

To evaluate the impact of soil moisture on LoRa performance, the soil in the sandbox was saturated to the highest possible volumetric water content (VWC) possible, using a long drip pipe evenly distributed in circles across the surface of the soil and along the boundary of the testbed. We start LoRa experiments once the water potential reached field capacity, and we continue them until the soil moisture reaches the wilting point. The soil moisture readings from the data logger are recorded in centibars (cB) and converted to VWC using the empirical conversion curve in [14]. We report two groups of results from two soil moisture levels: wet (15 cB or 37% VWC) and dry (51 cB or 17% VWC).

2) Outdoor Testbed: In addition, we perform outdoor testbed experiments with 433 MHz dipole and wideband planar antennas buried at a depth of 20 cm. The outdoor testbed allows a maximum distance of 115 m, which helps validate the channel path loss model. We also maintain the height of the aboveground node at 1.66 m, and the inter-node

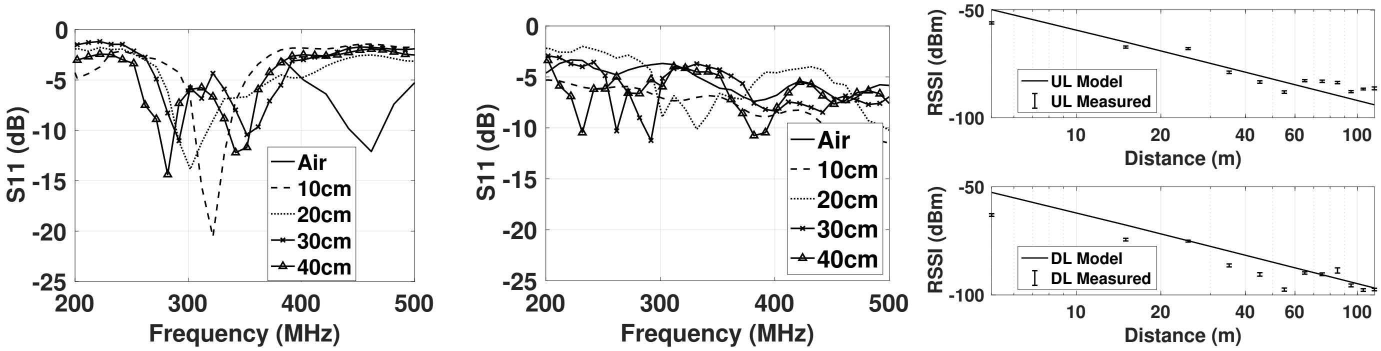

(a) (b) (c)

Fig. 4: The return loss of (a) 433MHz dipole antenna and (b) micropatch planar antenna in sandy soil for over-the-air and at different burial depths. (c) Theoretical and measured RSSI for uplink (top) and downlink (bottom) in silty clay loam soil in the outdoor testbed.

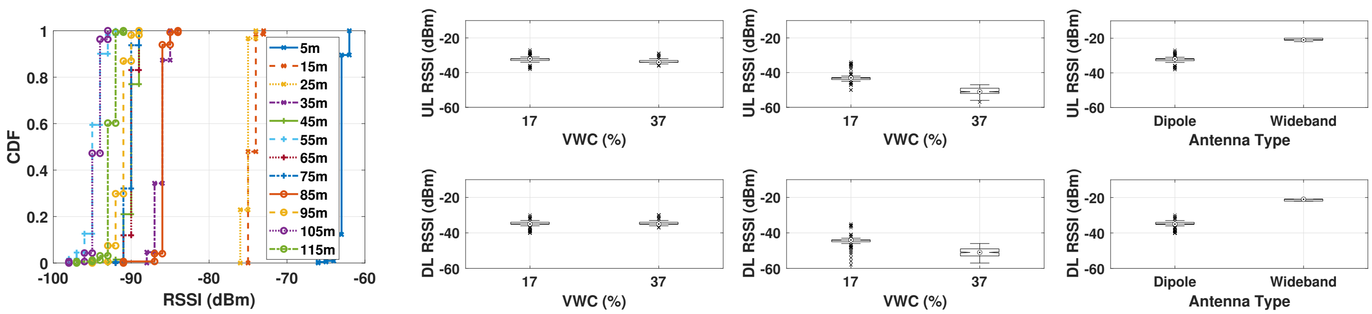

(a) (b) (c) (d)

Fig. 5: (a) CDF of the RSSI at each measurement distance in the outdoor testbed. (b) The RSSI using dipole antennas for uplink and downlink at 10 cm buried depth, (c) the RSSI using dipole antennas for uplink and downlink at 40 cm burial depth, and (d) the RSSI using dipole and wideband antennas for uplink and downlink at 10 cm burial depth.

distance was varied by moving the AG node in $10\,\mathrm{m}$ intervals from $5\,\mathrm{m}$ to $115\,\mathrm{m}$. The outdoor testbed consists of silty clay loam soil, providing a different soil type for analysis. The soil-related parameters associated with the indoor and outdoor testbeds are shown in Table I.

B. Measurement Results

1) Antenna Return Loss Measurements: The return loss (S11) of the dipole and wideband planar antennas buried in sandy soil is first measured for different deployment depths and in the air using a vector network analyzer (VNA), which are presented in Figs 4a-4b. The return loss of the 3 dB gain dipole antenna at 433 MHz in the air, and at 10, 20, $40\,\mathrm{cm}$ depths are -9.8, -1.8, -3.2, and -2.5 dB, respectively. For example, the return loss degradation will translate into a 4.7 dB loss in transmit power at $10\,\mathrm{cm}$, when the power of the transmitter is 20 dBm. Similar impact can also be observed from the micropatch antenna measurement. This addresses the importance of considering the antenna return loss in the LoRa performance analyses and experimental characterizations.

2) Channel Model Validation: We perform experiments using the outdoor testbed by transmitting 200 LoRa packets in uplink and downlink directions. The received signal strength indicator (RSSI) and signal to noise ratio (SNR) information are collected from the transmissions. We validate the path loss model described in Section II. The variables ϵ, ϵ' and ϵ'' used in the Peplinski dielectric mixing model are calculated based on the values presented in Table I. The soil parameter is utilized to reflect the physical soil setting in the experiment to evaluate the model's accuracy.

Fig. 4c demonstrates the range test performed in the outdoor testbed. The downlink and uplink RSSI values are recorded at each measurement distance. It can be observed that the UL and DL RSSIs derived based on the models in Section II have a good fit with the measurement results. More specifically, the R-squared values are 0.87 and 0.89, and the mean squared error (MSE) is 22.39 and 33.48 for UL and DL, respectively. It is worth noting that the experiments are performed in an open space with buildings and trees on the two sides of the area, at around 15m from each side, which could introduce reflections and cause slight deviations from the model. Also, the physical soil surface is not ideal, which can introduce additional loss due to scattering, leading to inaccuracies in refraction loss calculation at the soil-air interface. To show the fading impacts, in Fig. 5a, the deviation of the experimental measurements from the empirical and the theoretical means are shown . The CDF shows that the random noise in the channel is low at the measurement time, where more than 90% of the measured values are centered around the mean. Based on the analysis of the range test, we can see that the model can predict the received power for uplink or downlink channels with given physical settings and parameters.

3) Impacts of Soil Moisture: The impacts of soil moisture are studied using the indoor testbed with sandy soil. In these experiments, the UG nodes use dipole antennas to communicate with the AG node at a fixed distance, as mentioned above. In Fig. 5b, the UL and DL RSSIs at a 10 cm depth are shown. The received power reduces by 1.15 dB, on average, when the VWC increases from 17% to 37%. In this case, we believe that due to the porosity and bulk density of sandy soil, soil water quickly drains down, and the sandy soil did not hold the bound water. Therefore, the attenuation caused by soil water content is not strong at 10 cm depth.

Comparing the UL and DL RSSI in Fig. 5b, we observe that the uplink has a larger RSSI than the downlink. This difference is explained by the refraction loss difference at the soil-air interface and follows the model and the measurement done in the outdoor range test. In Fig. 5c, the UL and DL RSSIs at a 40 cm depth are shown. The reduction in received power at higher depth and higher soil moisture levels is more pronounced. The uplink and downlink RSSI decreases with soil moisture by 8.35 and 7.14 dB, respectively. Comparing Fig. 5b and 5c, the impact of buried depth on the path loss is also shown. A 10.25 dB loss on average is observed when the depth increases from 10 cm to 40 cm.

4) Impact of Underground Antennas: Next, we investigate the impact of underground antenna type on the uplink and downlink received power with the dipole and wideband antennas deployed in the indoor testbed. The uplink and downlink RSSIs are compared in Fig. 5d, where the buried depth is 10 cm, and the soil moisture level is dry. It can be observed that the wideband antenna has an average of 11 dB better RSSI. This difference is caused jointly by the lower gain and higher return loss of the dipole antennas . The wideband antenna would be preferred to be used in underground nodes to increase the channel link budget in (1), such that one can extend the communication range. The antenna return loss has the same impact on both uplink and downlink channels. The difference between uplink and downlink mainly comes from the refraction loss difference .

V. Conclusion

In this paper, we study the impact of soil medium and its properties on the LoRa modulation in UG channels. In particular, we present empirical measurement results and analysis of LoRa under different soil types, soil moisture conditions, and antenna types. By leveraging UG channel models, we derive the predictions of the performance of LoRa under varying conditions. The following steps of our study will include power consumption analysis and develop adaptive LoRa systems for practical applications, such as intelligent monitoring and smart agriculture.

VI. Acknowledgments

This work is supported in part by NSF projects CNS-1619285, CNS-1731833, and the Daugherty Water for Food Global Institute at the University of Nebraska.

References

[1] I. Akyildiz, Z. Sun, and M. Vuran, “Signal propagation techniques for wireless underground communication networks,” *Physical Communication*, vol. 2, no. 3, pp. 167–183, 2009.

[2] M. C. Vuran, A. Salam, R. Wong, and S. Irmak, “Internet of underground things in precision agriculture: Architecture and technology aspects,” *Ad Hoc Networks*, vol. 81, pp. 160–173, dec 2018. [Online]. Available: https://doi.org/10.1016%2Fj.adhoc.2018.07.017

[3] M. Hardie and D. Hoyle, “Underground wireless data transmission using 433-mhz lora for agriculture,” *Sensors*, vol. 19, no. 19, p. 4232, 2019.

[4] K. Lin and T. Hao, “Experimental link quality analysis for lora-based wireless underground sensor networks,” *IEEE Internet of Things Journal*, 2020.

[5] X.-f. Wan, Y. Yang, J. Cui, and M. S. Sardar, “Lora propagation testing in soil for wireless underground sensor networks,” in *2017 Sixth Asia-Pacific Conference on Antennas and Propagation (APCAP)*. IEEE, 2017, pp. 1–3.

[6] X.-F. Wan, Y. Yang, X. Du, and M. S. Sardar, “Design of propagation testnode for lora based wireless underground sensor networks,” in *2017 Progress in Electromagnetics Research Symposium-Fall (PIERS-FALL)*. IEEE, 2017, pp. 579–583.

[7] Z. Sun and I. F. Akyildiz, “Connectivity in wireless underground sensor networks,” in *2010 7th Annual IEEE Communications Society Conference on Sensor, Mesh and Ad Hoc Communications and Networks (SECON)*. IEEE, 2010, pp. 1–9.

[8] X. Dong, M. Vuran, and S. Irmak, “Autonomous precision agriculture through integration of wireless underground sensor networks with center pivot irrigation systems,” *Ad Hoc Networks*, vol. 11, no. 7, pp. 1975–1987, 2013.

[9] X. Dong and M. Vuran, “Impacts of soil moisture on cognitive radio underground networks,” in *2013 1st International Black Sea Conference on Communications and Networking, BlackSeaCom 2013*, 2013, pp. 222–227.

[10] A. Semtech, “120022, lora modulation basics, may, 2015.”

[11] Proakis, *Digital Communications, 5th Edition*. McGraw Hill, 2007.

[12] J. A. Stratton, “Electromagnetic theory, vol. 33,” 2007.

[13] N. R. Peplinski, F. T. Ulaby, and M. C. Dobson, “Dielectric properties of soils in the 0.3-1.3-ghz range,” *IEEE Transactions on Geoscience and Remote Sensing*, vol. 33, no. 3, pp. 803–807, 1995.

[14] A. Salam, M. C. Vuran, and S. Irmak, “Di-sense: In situ real-time permittivity estimation and soil moisture sensing using wireless underground communications,” *Computer Networks*, vol. 151, pp. 31–41, mar 2019.

[15] A. Salam, M. C. Vuran, X. Dong, C. Argyropoulos, and S. Irmak, “A theoretical model of underground dipole antennas for communications in internet of underground things,” *IEEE Transactions on Antennas and Propagation*, vol. 67, no. 6, pp. 3996–4009, jun 2019.

[16] J. C. Liando, A. Gamage, A. W. Tengourtius, and M. Li, “Known and unknown facts of lora: Experiences from a large-scale measurement study,” *ACM Transactions on Sensor Networks (TOSN)*, vol. 15, no. 2, pp. 1–35, 2019.

[17] B. Reynders, W. Meert, and S. Pollin, “Range and coexistence analysis of long range unlicensed communication,” in *2016 23rd International Conference on Telecommunications (ICT)*. IEEE, 2016, pp. 1–6.

[18] B. Reynders and S. Pollin, “Chirp spread spectrum as a modulation technique for long range communication,” in *2016 Symposium on Communications and Vehicular Technologies (SCVT)*. IEEE, 2016, pp. 1–5.

[19] A. Silva and M. Vuran, “Communication with aboveground devices in wireless underground sensor networks: An empirical study,” in *IEEE International Conference on Communications*, 2010.

[20] A. Salam and M. C. Vuran, “Smart underground antenna arrays: A soil moisture adaptive beamforming approach,” in *IEEE INFOCOM 2017 - IEEE Conference on Computer Communications*. IEEE, may 2017. [Online]. Available: https://doi.org/10.1109%2Finfocom.2017.8056990

[21] S. Irmak, “Soil water content- and soil matric potential-based irrigation trigger values for different soil types,” 2019.

[22] J. H. Scott, “Electrical and magnetic properties of rock and soil,” US Geological Survey,, Tech. Rep., 1983.

[23] *Adafruit Feather M0 Radio with LoRa Radio Module*, https://cdn-learn.adafruit.com/downloads/pdf/adafruit-feather-m0-radio-with-lora-radio-module.pdf, Adafruit.

[24] *WATERMARK Soil Moisture Sensor - MODEL 200SS*, https://www.irrometer.com, Irrometer Company Inc.